Published in final edited form as:
Mol Cell. 2012 February 10; 45(3): 344–356. doi:10.1016/j.molcel.2012.01.002.

PCGF Homologs, CBX Proteins, and RYBP Define Functionally Distinct PRC1 Family Complexes

Zhonghua Gao[1,*], **Jin Zhang**[1,*], **Roberto Bonasio**[1], **Francesco Strino**[2], **Ayana Sawai**[1], **Fabio Parisi**[2], **Yuval Kluger**[2], and **Danny Reinberg**[1,#]

[1]Howard Hughes Medical Institute, New York University School of Medicine, Department of Biochemistry, New York, NY 10016, USA

[2]Department of Pathology and Yale Cancer Center, Yale University School of Medicine, New Haven, CT 06520, USA

Summary

The heterogeneous nature of mammalian PRC1 complexes has hindered our understanding of their biological functions. Here, we present a comprehensive proteomic and genomic analysis that uncovered six major groups of PRC1 complexes each containing a distinct PCGF subunit, a RING1A/B ubiquitin ligase, and a unique set of associated polypeptides. These PRC1 complexes differ in their genomic localization and only a small subset co-localize with H3K27me3. Further biochemical dissection revealed that the six PCGF-RING1A/B combinations form multiple complexes through association with RYBP or its homolog YAF2, which prevents the incorporation of other canonical PRC1 subunits such as CBX, PHC and SCM. Although both RYBP/YAF2- and CBX/PHC/SCM-containing complexes compact chromatin, only RYBP stimulates the activity of RING1B toward H2AK119ub1, suggesting a central role in PRC1 function. Knockdown of RYBP in ES cells compromised their ability to form embryoid bodies, likely because of defects in cell proliferation and maintenance of H2AK119ub1 level.

Introduction

Polycomb Group (PcG) genes were originally identified in *Drosophila melanogaster* as developmental regulators of body segmentation through Hox gene repression (Lewis, 1978; Struhl, 1981), and they are crucial for many biological processes in mammals, including stem cell maintenance and differentiation, and cancer (Jaenisch and Young, 2008; Margueron and Reinberg, 2011; Sparmann and van Lohuizen, 2006). PcG proteins assemble in multi-subunit nuclear complexes with various biochemical functions, including recognition and modification of histone post-translational modifications (PTMs) and chromatin compaction (Simon and Kingston, 2009). The two most studied PcG complexes are Polycomb Repressive Complex 1 (PRC1) and 2 (PRC2), which catalyze two repressive histone PTMs: monoubiquitination of histone H2A at lysine-119 (H2AK119ub1) and

[#]Corresponding author: danny.reinberg@nyumc.org.
[*]These authors contribute equally

ACCESSION NUMBERS

ChIP-seq data are deposited in the NCBI GEO database with accession number GSE34774.

methylation of histone H3 at lysine-27 (H3K27me), respectively (Margueron and Reinberg, 2011; Simon and Kingston, 2009).

Since their discovery, PRC1 and PRC2 have been the object of extensive biochemical investigation (Vidal, 2009), genetic dissection (Grimaud et al., 2006), and genomic analysis (Ringrose, 2007), which have unveiled the complexity and diversity of the mammalian counterparts of these protein complexes. Mammalian PRC1 complexes are very heterogeneous, because each of the *Drosophila* subunits has several homologs in the human genome, and they can associate in a combinatorial fashion. In *Drosophila*, the core PRC1 complex (Saurin et al., 2001; Shao et al., 1999) contains Polycomb (Pc), a chromodomain-containing protein that binds to H3K27me3 (Fischle et al., 2003; Min et al., 2003); dRing, the enzyme responsible for H2A ubiquitination (Wang et al., 2004); Posterior Sex Combs (Psc), responsible for chromatin compaction *in vitro* (Francis et al., 2004); and Polyhomeotic (Ph). Additional components are found associated with PRC1 in sub-stoichiometric amounts, such as the PcG protein Sex Comb on Midleg (Scm). The initial mammalian PRC1 (henceforth canonical PRC1) purified from HeLa cells contained various chromodomain proteins (CBX) homologous to Pc; enzymes similar to dRing, called RING1A and RING1B; three Ph homologs (PHC1–3); BMI1/PCGF4, one of 6 human Psc homologs, collectively known as Polycomb group RING fingers (PCGFs); and sub-stoichiometric amounts of SCMH1, an Scm homolog (Levine et al., 2002). Combinatorial association of these different PcG homologs likely give rise to functionally distinct PRC1 complexes in humans. In fact, purification of BcoR- and L3MBTL2-associated polypeptides identified different PRC1-related complexes that instead of PCGF4 contained NSPC1/PCGF1 and MBLR/PCGF6, respectively, together with other factors (Gearhart et al., 2006; Trojer et al., 2011).

Genetic evidence suggests that the canonical PRC1 is required for transcriptional repression (Simon and Kingston, 2009). Genome-wide target analysis in embryonic stem cells (ESCs) revealed that PRC1 and PRC2 complexes localize to the promoters of developmental regulators (Boyer et al., 2006; Lee et al., 2006), suggesting that one function of PRCs is to maintain ESC pluripotency through silencing of differentiation genes. One current model for PRC1 recruitment at target genes posits that H3K27me functions as a recruitment signal through binding of Pc/CBX (Simon and Kingston, 2009); however, cases of H3K27me-independent localization have also been reported (Pasini et al., 2007; Schoeftner et al., 2006; Trojer et al., 2011).

From a mechanistic perspective, two molecular functions have been attributed PRC1: chromatin compaction (Levine et al., 2002; Shao et al., 1999) and H2AK119 monoubiquitination (Wang et al., 2004). Some non-canonical PRC1, the BcoR complex and L3MBTL2 complex, also catalyze H2AK119 monoubiquitination (Gearhart et al., 2006; Trojer et al., 2011), and in addition, L3MTBL2 compacts chromatin *in vitro* (Trojer et al., 2011). With even more such complexes expected to exist, a systematic study is needed to clarify the physical inter-relationship among all PRC1 complexes, as well as their activities.

The most recent additions to the family of human PRC1 complex components are RING1/YY1-binding protein (RYBP) and its homolog YAF2 (Vidal, 2009). These proteins bind to RING1A/B and YY1 (Garcia et al., 1999; Kalenik et al., 1997), the mammalian homologue of *Drosophila* Pho that is required for recruitment of PRC1/2 to certain Polycomb Responsive Elements (PRE) in *Drosophila* (Simon and Kingston, 2009). Because of the potential interaction of RYBP/YAF2 with YY1, it has been proposed that RYBP/YAF2 might serve as mediators to bridge PRC1 to YY1 for their recruitment (Wilkinson et al., 2010; Woo et al., 2010); however, their precise role in the context of human PRC1 function remains unknown.

To clarify and distinguish the functions of the different mammalian PRC1 complexes, we have undertaken a comprehensive proteomic and genomic approach. All PRC1 complexes identified by our approach contain RING1A/B, but falls into 6 different groups based on which PCGF they contain. Genome-wide target analysis revealed that different PRC1 complexes have distinct genomic localizations, indicating the existence of a sophisticated recruitment program, which depends on the subunit composition of the individual complexes. Interestingly, RYBP or its homolog YAF2 are found in most PRC1 complexes except those containing CBXs, PHCs, and SCMs. Biochemical and genomic analyses demonstrated a critical role of RYBP in the function of PRC1, and depletion of RYBP in ESCs led to a defect in embryoid body formation, which correlated with compromised cell proliferation and loss of H2A monoubiquitination.

RESULTS

Proteomic profiling of the family of PRC1 complexes

To determine the composition of the various PRC1 complexes in human cells, we performed tandem affinity purification (TAP) from 293 T-REx cells stably expressing doxycycline-inducible NSPC1/PCGF1, MEL18/PCGF2, PCGF3, BMI1/PCGF4, PCGF5, MBLR/PCGF6, or RING1B, each fused with sequential N-terminal FLAG and HA tags (NFH). To minimize non-specific binding and other over-expression artifacts, we induced expression of the tagged proteins at levels comparable with their endogenous counterparts (Figure S1A). TAP immunoprecipitates were subjected to mass spectrometry (MS) to determine associated polypeptides (Figure 1A). Two central observations emerged from this initial analysis: 1) all PRC1 complexes contain RING1A and RING1B (Figure 1A, lanes 1–6), enzymes that catalyze H2AK119ub1, and 2) the critical determinant of PRC1 complex identity is the type of PCGF protein (Figure 1A, lanes 1–6, and see below). That is to say, all PCGFs were recovered in the RING1B TAP, but in each individual PCGF TAP, no other PCGF was found (Figure 1A, lanes 1–7), indicating that each PCGF pairs with RING1B in an exclusive manner. In turn, each PCGF associated with different polypeptides (Figure 1A, lanes 1–6), with the exception of PCGF2 and PCGF4, which appeared to form relatively similar complexes. Although some of the proteins identified by our proteomic analysis were already known as PRC1 components (Vidal, 2009), many had not been previously recovered. For example, TAPs for the previously uncharacterized PCGF3 and PCGF5 recovered AUTS2, FBRS and FBRSL1, which have no known relationship with PRC1 (Figure 1A, lanes 3 and 5). Some of the factors identified by MS were confirmed by western blotting (Figure S1B). In light of these results, we conducted a second round of TAPs for NFH-RYBP, -YAF2, -CBX2/4/6, and -PHC1–3. The network of interactions obtained through this extensive TAP-MS approach revealed the existence of six groups of PRC1 complexes (Figure 1A and 1C). To reflect the specific association of each PCGF with core PRC1 components and different sets of polypeptides, we will refer to these six groups of PRC1 complexes as PRC1.1, PRC1.2, PRC1.3, PRC1.4, PRC1.5, or PRC1.6 according to their PCGF subunit (PRC1.1 contains PCGF1, PRC1.2 contains PCGF2, and so on). The association of additional proteins with various PCGFs is for the most part exclusive, but they are all recovered from RING1B pull-down (Figure 1A, lane 7). The conclusion that PCGF determines distinct complexes is further supported by the results of immunoprecipitation (IP) experiments in 293T cells, showing that distinct PCGFs interact with their specific partners (Figure 1B). The presence of RING1A in all PRC1 complexes was also confirmed by co-IP (Figure S1C). As a specificity control, YY1, which was not recovered in our TAPs, did not interact with any of the PRC1 components tested (Figure 1B, and S1C).

In addition to RING1A/B, RYBP and YAF2 co-purified with all PCGFs (Figure 1A, lanes 1–6). The presence of RYBP in PRC1 complexes was further confirmed by co-IP experiments using RING1A, RING1B, RYBP, PCGF1, PCGF2, PCGF4, and PCGF6

antibodies (Figure 1B and S1C). Interestingly, the presence of RYBP or YAF2 in PRC1.2 and PRC1.4 complexes excluded canonical components, such as CBXs, PHCs, and SCMs (Figure 1A), consistent with the finding that CBX2 did not co-immunoprecipitate with RYBP (Figure 1B, left). This suggests that at least in the case of PRC1.2 and PRC1.4, two subtypes of complexes are formed, one with canonical PcG components (CBXs, PHCs and SCMs), and one with either RYBP or YAF2 (Figure 1A). RYBP and YAF2 are also mutually exclusive, given that TAP of RYBP did not recover YAF2 and vice versa (Figure 1A, lane 14 and 15). The widespread presence of RYBP and YAF2 indicates that they play a critical role in the function of PRC1 complexes. In fact, inclusion or exclusion of RYBP/YAF2 results in additional heterogeneity within the six PRC1 complex groups, as evidenced by glycerol gradient fractionation followed by MS analysis (Figure S2).

Although the above results were obtained in 293T-REx cells, some of the interactions, such as those identified by NFH-RING1B and NFH-PCGF1 TAPs, were verified by co-IP in murine ESCs (Figure S1D), suggesting that this intricate network of PRC1 complexes is conserved among different cell types and evolutionarily related organisms, and are not a peculiarity of the cell line or the affinity tags utilized in our experiments.

In summary, our proteomic analysis demonstrate the existence of an “extended” family of PRC1 complexes in human cells (Figure 1C), characterized by the conserved presence of a RING1A/B (Figure 1A and S1C) subunit, which likely confer to all members the H2A ubiquitinating activity. The PRC1 family can be divided into at least 6 groups, which we refer to as PRC1.1–1.6 (Figure 1C), based on the identity of the PCGF subunit, and within each group further complexity can be revealed by more in-depth biochemical analysis (see below). RYBP (or its homolog YAF2) associates with all groups of PRC1 complexes, suggesting a central role in PRC1 function. However, at least in the case of PRC1.2 and PRC1.4, incorporation of RYBP/YAF2 is accompanied by the loss of other protein subunits (CBXs, PHCs, SCMs). This variety of complexes and their heterogeneous composition likely provides a platform for the diverse functions of PRC1 *in vivo*.

Different PCGFs occupy distinct genomic loci

Having profiled the subunit composition of the different PRC1 complexes, we sought to investigate their genomic localization by chromatin IP followed by deep sequencing (ChIP-seq). We performed ChIP with anti-HA antibodies (HA ChIP-seq) on extracts from 293T-REx cell lines after inducing expression of NFH-RING1B, -RYBP, -PCGF1, -PCGF2, -PCGF4, -PCGF5, -PCGF6 and -CBX2. Because H3K27me3 and H2AK119ub1 are commonly associated with Polycomb function (Simon and Kingston, 2009), we also performed ChIP for these chromatin marks.

Consistent with the role of PRC1 in regulating gene expression, all analyzed PRC1 components were predominantly found in the 10 kb region surrounding transcriptional start sites (TSS) (Figure S3), which prompted us to narrow our subsequent analyses to these regions.

Confirming our biochemical observations, we found several examples of promoters bound exclusively—or predominantly—by only one PCGF (Figure 2A). As expected, most of these loci were also bound by RING1B and RYBP, regardless of which PCGF was present (Figure 2A). To extend this observation to the whole genome, we identified significantly ($P<0.01$) enriched regions (SERs) using an in-house developed peak caller (Asp et al., 2011) and calculated the percentage of PRC1 target genes that contained SERs for RING1B and PCGFs. SERs for RING1B were found at most (58%–74%) genes targeted by PCGF1/2/4/5/6 (Figure 2B, highlighted box). The fraction of genes targeted by more than one PCGF was much smaller, ranging from 12% to 31% (Figure S4A–B), consistent with

our biochemical observations that RING1B is a key component of all PRC1 groups, whereas each PCGF forms distinct complexes (Figure 1A and 1C).

Despite some overlap in gene targets by different PCGFs, the functional terms associated with PCGF-enriched regions according to GREAT (McLean et al., 2010) were very different (Figure 2C), suggesting that the chromatin distribution of each PCGF reflects functional differences. PCGF1 target genes were enriched for GO terms including “cell junction organization” and “striated muscle cell differentiation”; PCGF2 targets were enriched for terms such as “epithelial cell differentiation” and “embryonic pattern specification”; PCGF4 targets were enriched for terms related with translation and metabolism; PCGF5 targets were related with mouse phenotypes like “decreased startle reflex” and “abnormal muscle relaxation”; and PCGF6 targets were enriched for mouse phenotype like “abnormal vaginal opening/morphology”.

To ensure that the NFH-tagged PRC1 components recapitulate the chromatin distribution of their endogenous counterparts, ChIP were also performed using antibodies against RING1B, RYBP, PCGF4 and CBX2 (endogenous ChIP-seq) in 293T-REx cells. Distribution profiles for endogenous PRC1 components, at many locations, mirrored the profiles that we obtained by HA ChIP-seq (Figure S4C).

CBX2-containing PRC1.2 and PRC1.4 accumulate at H3K27me3-rich regions

Because a popular mechanistic model for PRC1 recruitment envisions a central role for H3K27me3, we analyzed the correlation between the presence of this chromatin mark and binding of different PRC1 complexes. Only a small subset of PRC1 targets overlapped with H3K27me3-rich regions, and those were typically bound by complexes containing CBX2, PCGF2, and/or PCGF4 (Figure 2A and 3A). This observation is in contrast with the extensive overlap between RING1B and H3K27me3 reported in ESCs (Boyer et al., 2006; Ku et al., 2008), but consistent with other studies that reported H3K27me3-independent recruitment of PRC1 to chromatin (Pasini et al., 2007; Schoeftner et al., 2006; Trojer et al., 2011). PRC1.1, PRC1.5 and PRC1.6 SERs were mostly devoid of H3K27me3 (Figure 2A and 3A), and even among PRC1.2 and 1.4 SERs, the majority was devoid of any discernible H3K27me3 signal, which was almost exclusively detected in CBX2 SERs (Figure 3A). Consistent with this observation, a correlation study of the top 1000 RING1B SERs revealed distinct clusters of PRC1 components and a preferential association of H3K27me3 with CBX2 (Figure 3B). In fact, negative Pearson correlation coefficients between the ChIP-seq signal for PCGF1, 5, and 6 and that of H3K27me3 suggest that this mark may be slightly depleted from regions bound by PRC1.1, PRC1.5, and PRC1.6 (Figure 3B). The difference in H3K27me3 density between the top 50 SERs co-occupied by RING1B and each PCGF was also evident when we measured the normalized number of H3K27me3 reads (Figure 3C). In keeping with this, the distribution of L3MBTL2 (a PRC1.6 component) in K562 cells showed no correlation with H3K27me3 (Trojer et al., 2011).

We conclude that H3K27me3-rich regions are mostly occupied by PRC1.2 and PRC1.4, possibly via the interaction of CBX2 or other CBX proteins with H3K27me3 (Bernstein et al., 2006; Kaustov et al., 2011). This conclusion is consistent with our biochemical data that only PRC1.2 and PRC1.4 associate with CBXs, which is known to bind the H3K27me3 mark.

In contrast to H3K27me3, we found H2AK119ub1 enriched on SERs for all PCGFs (Figure 2A). However, we noted a similarity in the distribution of RYBP and H2AK119ub1 ChIP-seq signal (Figure 2A and 3E) and we found that within the top RING1B (2000 for HA-tagged and 200 for endogenous) SERs, those also occupied by RYBP displayed increased

intensity of H2AK119ub1 ChIP-seq signal (Figure 3D), suggesting the possibility that RYBP may facilitate the deposition of the ubiquitin mark in these regions (see below).

Differences in the local binding profile of RYBP and CBX proteins

According to our biochemical purification, PRC1 complexes contain either RYBP or CBXs but not both (Figure 1A, lane 8–15). Therefore, we were surprised to find that RYBP and CBX2 are often found in the vicinity of the same genes (Figure 2A) and that the distributions of these two proteins on chromatin seemed correlated (Figure 3B). However, we noticed that in many cases their binding profile to the same promoter differed greatly (Figure 3E). For example, at the *CCND2* promoter, CBX2 accumulates upstream of the broad RYBP peak, with minimal overlap. Similarly, on the *RUNX1* locus, although the bound regions of RYBP and CBX2 overlap partially, their peak shapes are quite different (Figure 3E). These differences would not have been detected by the gene target and genome-wide correlation analyses, which function on relatively large genome windows. To generalize this observation we analyzed the extent of overlap at the single nucleotide level between all RING1B-, PCGF2-, PCGF4- and RYBP-enriched regions that co-occupied with CBX2 (Figure 3F, bottom). Most of the RYBP-enriched regions overlap for less than 30% with CBX2-enriched regions, whereas a majority of PCGF2- and PCGF4-enriched regions overlap by 80% or more with CBX2. This suggests that at many promoters RYBP- and CBX-containing PRC1 complexes (Figure 3F top) co-exist by binding to adjacent yet separate regions. Importantly, this is not the case for RING1B and other PCGFs. Thus, although RYBP and CBX form mutually exclusive complexes, these complexes at times occupy the same genomic regions, but with distinct binding profiles.

Further characterization of PRC1.2/1.4 complexes

To better decipher the relationship between RYBP/YAF2 and the other subunits in the PRC1.2 and PRC1.4 complexes, we fractionated RING1B-containing complexes by differential centrifugation on a 15% – 35% glycerol gradient (Figure S2A). After a major peak in fraction 5 to 7, RING1B and PCGF4 were present throughout the gradient, whereas the distribution of RYBP/YAF2 and CBX4/CBX8 did not overlap (Figure 4A). This result confirmed that RYBP/YAF2 and CBX4/CBX8 form separate yet stable complexes with RING1B and PCGF4, as suggested by the proteomic analysis (Figure 1A, lanes 8–15). IPs of FLAG-purified RING1B complexes confirmed that RYBP and PHC3 do not interact with each other, although they both interact with RING1B (Figure 4B). Consistent with the proteomic results (Figure 1A), CBX4 co-immunoprecipitated with PHC3 (Figure 4B).

Our finding that RING1A/B, PCGF4, or PCGF2 form independent complexes with RYBP or YAF2, distinct from the canonical PRC1 complex, is consistent with the report that CBX7 (one of the PRC1-related CBX proteins) and RYBP bind to the same surface on the C-terminal domain of RING1B (Wang et al., 2010). Indeed, RYBP inhibited in a dose-dependent manner binding of CBX8 to RING1B (Figure 4C), suggesting that, RYBP and probably its homolog YAF2 compete for the same RING1A/B binding site with CBXs, and are potentially required at different times or for different aspects of PRC1 function (Figure 4D).

Functional comparison of RYBP- and CBX/PHC-containing PRC1 complexes

How PRC1 complexes enforce transcriptional repression remains poorly understood. Proposed mechanisms include compaction of chromatin and placement of a repressive mark, H2AK119ub1 (Simon and Kingston, 2009). We decided to focus on PRC1.4 and sought to determine how inclusion or exclusion of its different subunits affects its abilities to compact chromatin and to catalyze H2AK119ub1.

We isolated PRC1.4 by FLAG-purification from NFH-PCGF4-containing extracts and separated the complexes containing RYBP/YAF2 ("Fractions RYBP/YAF2") or CBX/PHC/SCM ("Fractions CBX/PHC") through differential centrifugation (Figure 5A). Incubation of either complex with a nucleosomal array caused a comparable shift of the array toward high molecular weight fractions in sucrose gradients (Figure 5B), suggesting that the shift mediated by PRC1.4 is not affected by the presence or absence of RYBP, CBX2 and PHC3. No difference were observed when the nucleosomal arrays were reconstituted with recombinant or native histones (Figure 5B), consistent with the observation that histone PTMs are not required for PRC1-mediated compaction (Francis et al., 2004). Recombinant PCGF4 did not affect the migration of the arrays on the gradient, whereas L3MBTL2 shifted it, consistent with our previous findings (Trojer et al., 2011). Electron microscopy (EM) analysis showed that the normal "beads on a string" morphology of nucleosomal arrays was converted to a more compacted structure upon pre-incubation with both complexes, albeit the one containing CBX/PHC/SCMs showed a slightly more closed structure (Figure 5C).

To test if the *in vitro* chromatin compaction activity of these PRC1 complexes recapitulates *in vivo* phenomena, an *in situ* chromatin accessibility assay was performed on several PRC1-bound loci. The high rate of nuclease protection showed that three of these loci (*C16ORF5*, *CCND2* and *RUNX1*) adopt a compacted chromatin state (Figure S5), similar to that of known compacted loci such as *RHO* and *SYN1*. Therefore, at least at a subset of PRC1 target loci, chromatin is in a compacted configuration.

We next asked whether the presence of the RYBP versus CBX/PHC subunits affected the ubiquitinating activity of PRC1.4 with reconstituted complexes purified from insect cells (Figure 5D, left). To our surprise, RYBP-containing RING1B-PCGF4 complexes exhibited stronger enzymatic activity than those containing PHC2 and either CBX2 or CBX8 (Figure 5E). This was at least in part due to the dose-dependent stimulatory effect of RYBP on a preformed RING1B-PCGF4 heterodimer (Figure 5F). These data suggest that human RYBP stimulates the activity of RING1B on H2AK119.

RYBP is required for ESC differentiation, cell proliferation, and maintenance of H2AK119ub1 *in vivo*

So far, we have established RYBP as a major component of PRC1 family complexes and identified a group of previous uncharacterized complexes containing RYBP or YAF2, together with RING1A/B and PCGFs. We next asked what role RYBP might play in the context of a critical PRC1 function: the regulation of ESC pluripotency and differentiation. After 9 days of *in vitro* differentiation, the deletion of RYBP caused abnormalities in the development of embryoid bodies (EBs) as evidenced by the absence of central cavities (Figure 6A), which were present in 51.1 ± 22.2% of control but only in 5.2 ± 6.6% of RYBP knockdown ESCs (Figure 6B). Knockdown of RYBP did not seem to impact the pluripotent state of the ESCs, as judged by expression levels of pluripotency markers (Figure 6C, top), but instead inhibited the induction of specific differentiation markers, especially of the endodermal and mesodermal lineage, such as *Gata4*, *Gata6*, *Mixl1*, and *Brachyury* (Figure 6C, bottom). No difference was observed in the expression levels of *Fgf5* and *Nestin*, two ectoderm markers (Figure 6C, bottom). This is consistent with the deficiency in central cavity formation during EB development from RYBP knockdown ESCs (Figure 6A–B), and suggests that RYBP has an important role in the transcriptional changes that occur during differentiation.

To test whether RYBP has any effect on cell proliferation, which may explain the defect in EB differentiation, RYBP was targeted for silencing by shRNA in HEK 293 and ESCs. Cells deficient for RYBP displayed greatly decreased proliferative potential, compared with control (Figure 6D). Although levels of RING1B were unchanged, knockdown of RYBP in

HEK 293 cells led to a dramatic reduction in H2AK119ub1 level but no changes in H3K27me3 (Figure 6E). Together with our finding that RYBP-containing complexes have greater ubiquitinating activity than the canonical PRC1 (Figure 5E), these data suggest that RYBP-containing PRC1 complexes are responsible for the majority of the H2AK119ub1 repressive mark on chromatin.

DISCUSSION

Distinct group of PRC1 complexes and functions

Great efforts have been made to identify and characterize the mammalian equivalent(s) of *Drosophila* PRC1(Vidal, 2009). However, previous studies focused on only a few subunits for biochemical purifications and genome-wide characterization. With TAP analysis of a panel of PRC1 subunits, we have identified six groups of PRC1 complexes, PRC1.1–1.6, distinguished by the presence of a different member of the PCGF family. The presence of RYBP and YAF2 defines different complex subgroups, which, at least in the case of PRC1.2 and PRC1.4, exclude the presence of other subunits such as CBXs, SCMs, and PHCs. ChIP-seq revealed differences in the distribution of the analyzed PRC1 complexes in the promoter regions of annotated genes, suggesting distinct chromatin targets and biological functions for each PRC1 group, which is further supported by GO enrichment analysis of their target genes. Interestingly, PCGF5 targets were enriched for GO terms associated with neuronal functions (Figure 2C). Given that PCGF5 also co-purifies with proteins implicated in brain function, such as AUTS2, we speculate that PRC1.5 may have a specialized role in the brain.

The recruitment mechanisms of PRC1 complexes

The mechanism of the recruitment of mammalian PRC1 to target genes remains one of the fundamental questions in the field. In *Drosophila*, PREs function as *cis*-acting DNA sequences for recruitment of PRC1 and PRC2, which also requires *trans*-acting DNA binding factors, such as Pleiohomeotic (Pho) (Simon and Kingston, 2009). The genomic distribution of Pho overlaps substantially with that of PRC1 and PRC2, suggesting an important role in PRC1 and PRC2 recruitment (Kwong et al., 2008; Oktaba et al., 2008; Schuettengruber et al., 2009). Yet, despite the recent identification of two PRE-like elements in the mammalian genome (Sing et al., 2009; Woo et al., 2010), the role of the mammalian homolog of Pho, YY1, in PRC1 recruitment and function is far less clear than in flies. Sevearl models exist to explain how PRC1 and PRC2 are recruited to their target sites in mammals, including association with specific DNA-binding factors, binding to H3K27me3, and interactions with non-coding RNAs (Schuettengruber and Cavalli, 2009; Simon and Kingston, 2009). However, PRC1 has been often studied as a single entity, masking the complexity of its recruitment mechanism. With our description of different groups of PRC1 complexes with distinct genomic localizations, it becomes evident that one or more recruitment pathways must exist that differentiate among the various PRC1 groups. For example, CBX2 is targeted to genomic regions with enriched H3K27me3, and these regions are selectively co-occupied by PCGF2 or/and PCGF4 but not other PCGFs. Considering that PRC1.2 and PRC1.4 bear the closest resemblance with the canonical PRC1 complex, this observation fits well with the known link between H3K27me3 and PRC1; however, we also detected promoters bound by PCGF2 and PCGF4 that did not contain significant levels of H3K27me3, in which cases CBX2 was also missing. Taken together, these results suggest that H3K27me3 recognition is partially involved in the function of a subset of PRC1 complexes, and is mostly restricted to CBX-containing PRC1.2 and PRC1.4. Thus, H3K27me3-independent mechanisms must exist for the recruitment of PRC1.1, 1.3, 1.5, 1.6, as well as PRC1.2 and 1.4 devoid of CBXs. We recently showed that PRC1.6 occupies E2F6 binding sites (Trojer et al., 2011); it would be interesting to test the role of other

transcription factors and co-factors in recruiting PRC1 complexes. For example, MAX and MGA are associated with a subset of PRC1.6 complexes and they may recruit PRC1.6 to some target genes. In the case of PRC1.1, it is likely that BCL6 binding to target sequences may recruit a subset of PRC1.1 through the interaction of BcoR or BcoRL1 with BCL6 (Gearhart et al., 2006). Another potential mechanism for PRC1 recruitment is via RYBP/YAF2-YY1 interactions. Indeed, a recent study identified a region between *HOXD11* and *HOXD12* as a mammalian PRE, where a cluster of *cis*-acting YY1 binding sites and RYBP contribute to the recruitment of PcG proteins (Woo et al., 2010). Because we could not detect a stable association of YY1 with PRC1 in our study, it is possible that the interaction between YY1 and RYBP/YAF2 or other PRC1 component may be transient or require prior binding of YY1 to chromatin. Yet, the majority of the PRC1 complexes analyzed here lack polypeptides known to interact with sequence-specific DNA binding proteins. Given that non-coding RNAs interact at least with one PRC1 component (Yap et al., 2010) and that the EZH2 subunit of PRC2 interacts with non-coding RNAs (Margueron and Reinberg, 2011), we suggest that diverse mechanisms operate to recruit PRC1 complexes to target genes.

RYBP/YAF2-containing and CBXs/PHCs/SCMs-containing PRC1 complexes

Our TAPs (Figure 1A) and glycerol gradient analysis (Figure 4A and S2) unveiled a unique type of PRC1 complexes that contains RYBP or YAF2 along with RING1A/B and one of the six PCGFs. We demonstrate that RYBP/YAF2 forms stable ternary complexes with RING1B and each PCGF and that this association prevents binding of other common complex components, at least in the case of PRC1.2 and PRC1.4. In PRC1.4, RYBP and YAF2 are mutually exclusive with CBX, PHC, and SCM proteins (Figure 1A, and 4), components of the canonical PRC1 complex identified previously (Levine et al., 2002). Although both RYBP- and CBX-containing versions of PRC1.4 compact chromatin *in vitro*, the presence of RYBP has a unique stimulatory effect on the enzymatic activity on the RING1B-PCGF4 dimer, suggesting that different types of PRC1.4 may repress transcription through different mechanisms. Knockdown of RYBP led to the loss of H2AK119ub1, reinforcing our conclusion that RYBP plays a critical role in regulating the E3 activity of RING1B. Similarly, in *Drosophila*, the dRAF complex containing dRing, Psc, and dKdm2 is more effective in catalyzing H2AK119ub1 than the canonical PRC1 complex both *in vitro* and *in vivo* (Lagarou et al., 2008). Although both subtypes of PRC1.2/1.4 complexes compact chromatin, the molecular mechanism may be different. It has been suggested that CBXs are responsible for chromatin compaction (Grau et al., 2010), instead of PCGF4, one homolog of *Drosophila* Psc, which originally showed such activity (Francis et al., 2004). In CBX-less PRC1 complexes, RYBP may play the role to compact chromatin, possibly via its affinity to DNA (Neira et al., 2009). Thus, further experiments are needed to carefully examine the influence of specific associated factors on the activities of the distinct PRC1 complexes, and their impact on PRC1-mediated transcriptional repression.

Experimental Procedures

Affinity purification, glycerol gradient and protein identification

Cells were induced by Doxycycline for 24 hours. Nuclear extracts (NE) were prepared as previously described (Dignam et al., 1983) with modifications. A detailed description is in the Supplemental Information.

ChIP-seq

All ChIP-seq experiments for PRC1 components were done using an HA antibody in 293T-REx cells expressing NFH-PRC1 components or endogenous antibodies in 293 T-REx cells stably transfected with a control vector. The procedure is described in details in Supplemental Information.

Lentiviral shRNAs

Packaging plasmids were co-transfected using lipofectamine 2000 (Invitrogen) with short hairpin RNA constructs for targeting both human and mouse RYBP (Open Biosystems). Stable knockdown in TT2 or HEK 293 cells were selected with 1 μg/ml puromycin.

In vitro Chromatin Compaction, Sucrose Gradients and EM

These experiments were performed as previously described (Trojer et al., 2007). Briefly, reconstituted nucleosomal arrays were incubated with isolated complexes at room temperature for 35 min, and then loaded onto a 4.5 ml 10–30% sucrose gradient, followed by centrifugation at 22, 000 RPM in a SW60Ti rotor (Beckman) at 4 °C for 16 hours. The resulting samples were fractionated every 330 μl, and examined by agarose gel. Chromatin samples in factions of interest were fixed with 0.6 % glutaraldehyde for 30 min on ice, and then processed for EM as described (Li et al., 2010).

In vitro H2A ubiquitination assays

Assays were performed as previously described (Wang et al., 2004) with modifications. Briefly, in the presence of 100 nM E1(Boston Biochem), 500 nM UbcH5c (Boston Biochem), 10 μM HA-ubiquitin (Boston Biochem), 5 mM ATP, and 2 μl of 10 × ubiquitination reaction buffer (500 mM Tris-HCl, pH 7.5, 50 mM $MgCl_2$, 10 mM DTT), reactions were assembled with reconstituted oligonucleosomes (~2.5 μg) and purified complexes or proteins in a total volume of 20 μl. After 2 hour incubation at 37 °C, the reactions were stopped by boiling in SDS sample buffer, and then resolved on SDS-PAGE, followed by immunoblotting.

Supplementary Material

Refer to Web version on PubMed Central for supplementary material.

Acknowledgments

We thank B. Bernstein, R. Koche, and other members of the Bernstein lab for great advice and helpful discussion on ChIP-seq; G. Felsenfeld for providing insulator sequences; V. Bardwell and C. Fry for providing reagents; D. Beck for vector construction; T. Iwahara and W. Tee for providing RT primers; H. Zheng for MS analysis; and P. Trojer for comments on the manuscript. This work is supported by grants from the National Institute of Health (GM-64844 and R37-37120), and the Howard Hughes Medical Institute to D.R.. R.B. was supported by a Helen Hay Whitney Foundation post-doctoral fellowship. F.P. and Y.K. were partially supported by the Yale SPORE in Skin Cancer funded by the National Cancer Institute (P50-CA121974, R. Halaban, PI). F.S. was supported by the American-Italian Cancer Foundation (Post-Doctoral Research Fellowship).

References

Asp P, Blum R, Vethantham V, Parisi F, Micsinai M, Cheng J, Bowman C, Kluger Y, Dynlacht BD. Genome-wide remodeling of the epigenetic landscape during myogenic differentiation. P Natl Acad Sci USA. 2011; 108:E149–E158.

Bernstein E, Duncan EM, Masui O, Gil J, Heard E, Allis CD. Mouse polycomb proteins bind differentially to methylated histone H3 and RNA and are enriched in facultative heterochromatin. Molecular and Cellular Biology. 2006; 26:2560–2569. [PubMed: 16537902]

Boyer LA, Plath K, Zeitlinger J, Brambrink T, Medeiros LA, Lee TI, Levine SS, Wernig M, Tajonar A, Ray MK, et al. Polycomb complexes repress developmental regulators in murine embryonic stem cells. Nature. 2006; 441:349–353. [PubMed: 16625203]

Dignam JD, Lebovitz RM, Roeder RG. Accurate transcription initiation by RNA polymerase II in a soluble extract from isolated mammalian nuclei. Nucleic Acids Res. 1983; 11:1475–1489. [PubMed: 6828386]

Fischle W, Wang YM, Jacobs SA, Kim YC, Allis CD, Khorasanizadeh S. Molecular basis for the discrimination of repressive methyl-lysine marks in histone H3 bv Polvcomb and HP1 chromodomains. Gene Dev. 2003; 17:1870–1881. [PubMed: 12897054]

Francis NJ, Kingston RE, Woodcock CL. Chromatin compaction by a polycomb group protein complex. Science. 2004; 306:1574–1577. [PubMed: 15567868]

Garcia E, Marcos-Gutierrez C, del Mar Lorente M, Moreno JC, Vidal M. RYBP, a new repressor protein that interacts with components of the mammalian Polycomb complex, and with the transcription factor YY1. Embo J. 1999; 18:3404–3418. [PubMed: 10369680]

Gearhart MD, Corcoran CM, Wamstad JA, Bardwell VJ. Polycomb group and SCF ubiquitin ligases are found in a novel BCOR complex that is recruited to BCL6 targets. Mol Cell Biol. 2006; 26:6880–6889. [PubMed: 16943429]

Grau DJ, Antao JM, Kingston RE. Functional dissection of Polycomb repressive complex 1 reveals the importance of a charged domain. Cold Spring Harb Symp Quant Biol. 2010; 75:61–70. [PubMed: 21502414]

Grimaud C, Negre N, Cavalli G. From genetics to epigenetics: the tale of Polycomb group and trithorax group genes. Chromosome Res. 2006; 14:363–375. [PubMed: 16821133]

Jaenisch R, Young R. Stem cells, the molecular circuitry of pluripotency and nuclear reprogramming. Cell. 2008; 132:567–582. [PubMed: 18295576]

Kalenik JL, Chen D, Bradley ME, Chen SJ, Lee TC. Yeast two-hybrid cloning of a novel zinc finger protein that interacts with the multifunctional transcription factor YY1. Nucleic Acids Res. 1997; 25:843–849. [PubMed: 9016636]

Kaustov L, Hui OY, Amaya M, Lemak A, Nady N, Duan SL, Wasney GA, Li ZH, Vedadi M, Schapira M, et al. Recognition and Specificity Determinants of the Human Cbx Chromodomains. J Biol Chem. 2011; 286:521–529. [PubMed: 21047797]

Ku M, Koche RP, Rheinbay E, Mendenhall EM, Endoh M, Mikkelsen TS, Presser A, Nusbaum C, Xie XH, Chi AS, et al. Genomewide Analysis of PRC1 and PRC2 Occupancy Identifies Two Classes of Bivalent Domains. Plos Genetics. 2008:4.

Kwong C, Adryan B, Bell I, Meadows L, Russell S, Manak JR, White R. Stability and dynamics of polycomb target sites in Drosophila development. PLoS Genet. 2008; 4:e1000178. [PubMed: 18773083]

Lagarou A, Mohd-Sarip A, Moshkin YM, Chalkley GE, Bezstarosti K, Demmers JA, Verrijzer CP. dKDM2 couples histone H2A ubiquitylation to histone H3 demethylation during Polycomb group silencing. Genes Dev. 2008; 22:2799–2810. [PubMed: 18923078]

Lee TI, Jenner RG, Boyer LA, Guenther MG, Levine SS, Kumar RM, Chevalier B, Johnstone SE, Cole MF, Isono K, et al. Control of developmental regulators by Polycomb in human embryonic stem cells. Cell. 2006; 125:301–313. [PubMed: 16630818]

Levine SS, Weiss A, Erdjument-Bromage H, Shao Z, Tempst P, Kingston RE. The core of the polycomb repressive complex is compositionally and functionally conserved in flies and humans. Mol Cell Biol. 2002; 22:6070–6078. [PubMed: 12167701]

Lewis EB. Gene Complex Controlling Segmentation in Drosophila. Nature. 1978; 276:565–570. [PubMed: 103000]

Li G, Margueron R, Hu G, Stokes D, Wang YH, Reinberg D. Highly compacted chromatin formed in vitro reflects the dynamics of transcription activation in vivo. Mol Cell. 2010; 38:41–53. [PubMed: 20385088]

Margueron R, Reinberg D. The Polycomb complex PRC2 and its mark in life. Nature. 2011; 469:343–349. [PubMed: 21248841]

McLean CY, Bristor D, Hiller M, Clarke SL, Schaar BT, Lowe CB, Wenger AM, Bejerano G. GREAT improves functional interpretation of cis-regulatory regions. Nat Biotechnol. 2010; 28:495–U155. [PubMed: 20436461]

Min JR, Zhang Y, Xu RM. Structural basis for specific binding of polycomb chromodomain to histone H3 methylated at Lys 27. Gene Dev. 2003; 17:1823–1828. [PubMed: 12897052]

Neira JL, Roman-Trufero M, Contreras LM, Prieto J, Singh G, Barrera FN, Renart ML, Vidal M. The transcriptional repressor RYBP is a natively unfolded protein which folds upon binding to DNA. Biochemistry. 2009; 48:1348–1360. [PubMed: 19170609]

Oktaba K, Gutierrez L, Gagneur J, Girardot C, Sengupta AK, Furlong EE, Muller J. Dynamic regulation by polycomb group protein complexes controls pattern formation and the cell cycle in Drosophila. Dev Cell. 2008; 15:877–889. [PubMed: 18993116]

Pasini D, Bracken AP, Hansen JB, Capillo M, Helin K. The polycomb group protein Suz12 is required for embryonic stem cell differentiation. Molecular and Cellular Biology. 2007; 27:3769–3779. [PubMed: 17339329]

Ringrose L. Polycomb comes of age: genome-wide profiling of target sites. Curr Opin Cell Biol. 2007; 19:290–297. [PubMed: 17481880]

Saurin AJ, Shao Z, Erdjument-Bromage H, Tempst P, Kingston RE. A Drosophila Polycomb group complex includes Zeste and dTAFII proteins. Nature. 2001; 412:655–660. [PubMed: 11493925]

Schoeftner S, Sengupta AK, Kubicek S, Mechtler K, Spahn L, Koseki HH, Jenuwein T, Wutz A. Recruitment of PRC1 function at the initiation of X inactivation independent of PRC2 and silencing. Embo Journal. 2006; 25:3110–3122. [PubMed: 16763550]

Schuettengruber B, Cavalli G. Recruitment of polycomb group complexes and their role in the dynamic regulation of cell fate choice. Development. 2009; 136:3531–3542. [PubMed: 19820181]

Schuettengruber B, Ganapathi M, Leblanc B, Portoso M, Jaschek R, Tolhuis B, van Lohuizen M, Tanay A, Cavalli G. Functional anatomy of polycomb and trithorax chromatin landscapes in Drosophila embryos. PLoS Biol. 2009; 7:e13. [PubMed: 19143474]

Shao Z, Raible F, Mollaaghababa R, Guyon JR, Wu CT, Bender W, Kingston RE. Stabilization of chromatin structure by PRC1, a Polycomb complex. Cell. 1999; 98:37–46. [PubMed: 10412979]

Simon JA, Kingston RE. Mechanisms of polycomb gene silencing: knowns and unknowns. Nat Rev Mol Cell Biol. 2009; 10:697–708. [PubMed: 19738629]

Sing A, Pannell D, Karaiskakis A, Sturgeon K, Djabali M, Ellis J, Lipshitz HD, Cordes SP. A vertebrate Polycomb response element governs segmentation of the posterior hindbrain. Cell. 2009; 138:885–897. [PubMed: 19737517]

Sparmann A, van Lohuizen M. Polycomb silencers control cell fate, development and cancer. Nat Rev Cancer. 2006; 6:846–856. [PubMed: 17060944]

Struhl G. A Gene-Product Required for Correct Initiation of Segmental Determination in Drosophila. Nature. 1981; 293:36–41. [PubMed: 7266657]

Trojer P, Cao AR, Gao Z, Li Y, Zhang J, Xu X, Li G, Losson R, Erdjument-Bromage H, Tempst P, et al. L3MBTL2 protein acts in concert with PcG protein-mediated monoubiquitination of H2A to establish a repressive chromatin structure. Mol Cell. 2011; 42:438–450. [PubMed: 21596310]

Trojer P, Li G, Sims RJ 3rd, Vaquero A, Kalakonda N, Boccuni P, Lee D, Erdjument-Bromage H, Tempst P, Nimer SD, et al. L3MBTL1, a histone-methylation-dependent chromatin lock. Cell. 2007; 129:915–928. [PubMed: 17540172]

Vidal M. Role of polycomb proteins Ring1A and Ring1B in the epigenetic regulation of gene expression. Int J Dev Biol. 2009; 53:355–370. [PubMed: 19412891]

Wang H, Wang L, Erdjument-Bromage H, Vidal M, Tempst P, Jones RS, Zhang Y. Role of histone H2A ubiquitination in Polycomb silencing. Nature. 2004; 431:873–878. [PubMed: 15386022]

Wang R, Taylor AB, Leal BZ, Chadwell LV, Ilangovan U, Robinson AK, Schirf V, Hart PJ, Lafer EM, Demeler B, et al. Polycomb group targeting through different binding partners of RING1B C-terminal domain. Structure. 2010; 18:966–975. [PubMed: 20696397]

Wilkinson F, Pratt H, Atchison ML. PcG recruitment by the YY1 REPO domain can be mediated by Yaf2. J Cell Biochem. 2010; 109:478–486. [PubMed: 19960508]

Woo CJ, Kharchenko PV, Daheron L, Park PJ, Kingston RE. A region of the human HOXD cluster that confers polycomb-group responsiveness. Cell. 2010; 140:99–110. [PubMed: 20085705]

Yap KL, Li SD, Munoz-Cabello AM, Raguz S, Zeng L, Mujtaba S, Gil J, Walsh MJ, Zhou MM. Molecular Interplay of the Noncoding RNA ANRIL and Methylated Histone H3 Lysine 27 by Polycomb CBX7 in Transcriptional Silencing of INK4a. Molecular Cell. 2010; 38:662–674. [PubMed: 20541999]

- All PRC1 complexes are divided into six groups characterized by six PCGF subunits
- These six groups of PRC1 complexes target different genes through distinct mechanisms
- RYBP/YAF2 form mutually exclusive PRC1 complexes with CBX/PHC/SCM proteins
- RYBP stimulates PRC1-mediated H2AK119ub1 and is essential for ESC differentiation

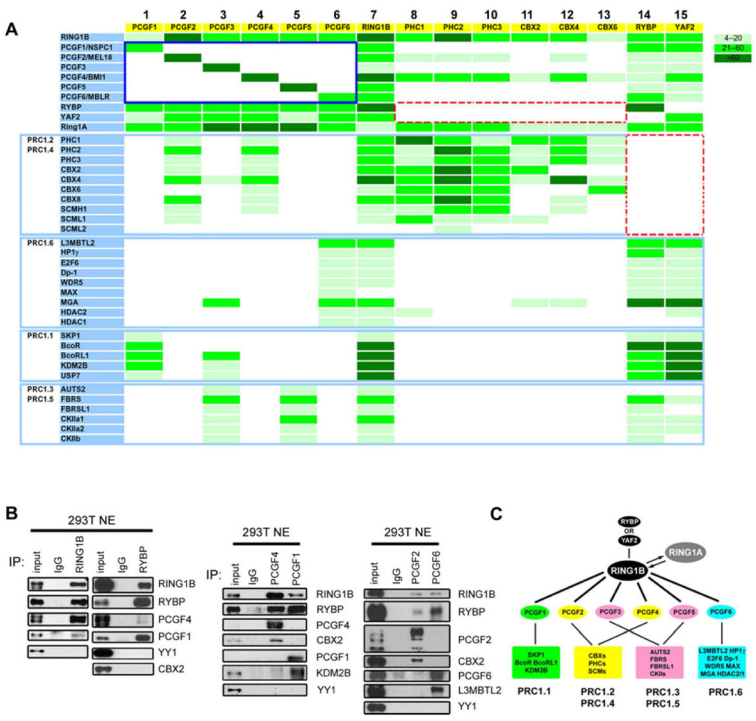

Figure 1. Proteomic analysis of PRC1 family complexes

A Heat map of PRC1-associated polypeptides. 293T-REx cells expressing the Flag-HA-tagged PRC1 subunit indicated at the top of the table were lysed and interacting polypeptides were recovered by sequential FLAG-HA affinity purification (TAP). The final eluate was subjected to Liquid chromatography-mass spectrometry (LC-MS), and the spectrum count of each protein is color-coded and displayed as a heatmap with more intense color representing more abundant species. Polypeptides are grouped according to which PCGF they associate with (referred to as PRC1.1–1.6, as indicated on the left).

B IP from 293T nuclear extracts (NE) using antibodies for RING1B, RYBP, PCGF4, PCGF1, PCGF2, and PCGF6. Bound proteins were resolved on SDS-PAGE and detected by western blotting for the indicated antigens.

C Schematic depiction of PRC1 family complexes. See text for details.

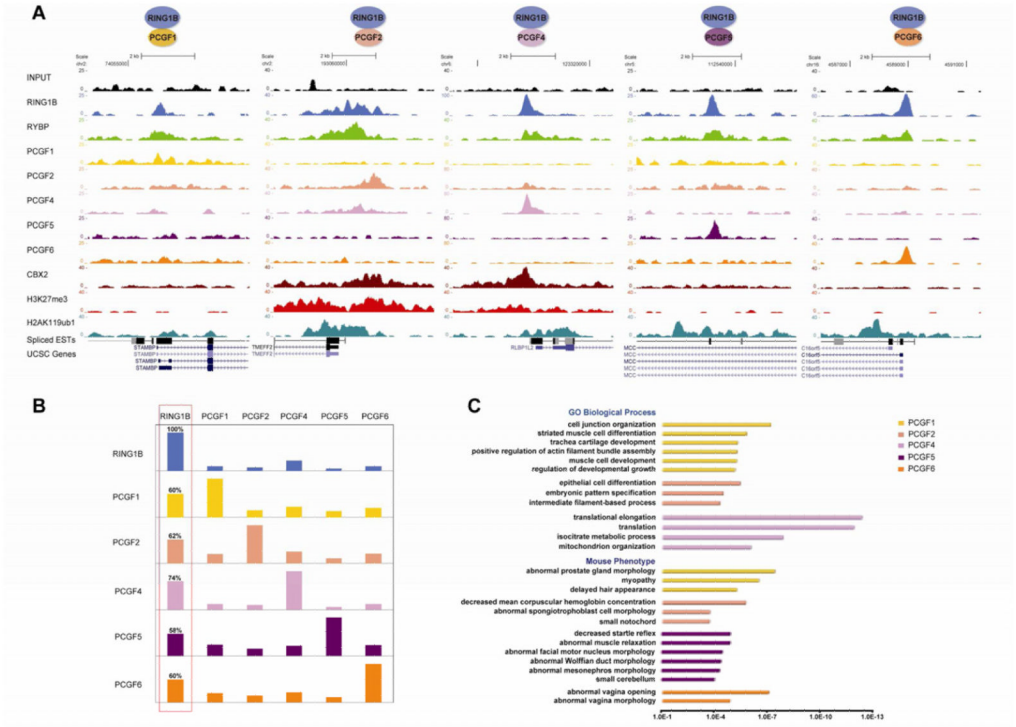

Figure 2. Different PCGF-containing PRC1 complexes are targeted to distinct genomic loci

A Read density for RING1B, PCGF1, PCGF2, PCGF4, PCGF5, PCGF6, CBX2, H3K27me3, and H2AK119ub1 ChIP-seq libraries at five loci. A cartoon representing the most enriched PRC1 complex detected at each locus is shown on top. The x axis corresponds to genomic locations, with the scale and genomic position indicated at the top of each panel. The y axis corresponds to the ChIP-seq signal intensity. Spliced ESTs and UCSC genes representation at each locus are shown on the bottom.

B Percentage of overlapping gene targets among RING1B and five PCGFs. Each row is normalized according to the total number of target genes identified for each protein. A red box highlights the percentage of gene targets of each protein that overlap with those of RING1B.

C GO biological process and mouse phenotype analysis of the targeted genomic regions identified in PCGF1, PCGF2, PCGF4, PCGF5 and PCGF6 ChIP-seq, using GREAT (McLean et al., 2010). The x axis (in logarithmic scale) corresponds to the binomial raw P-values.

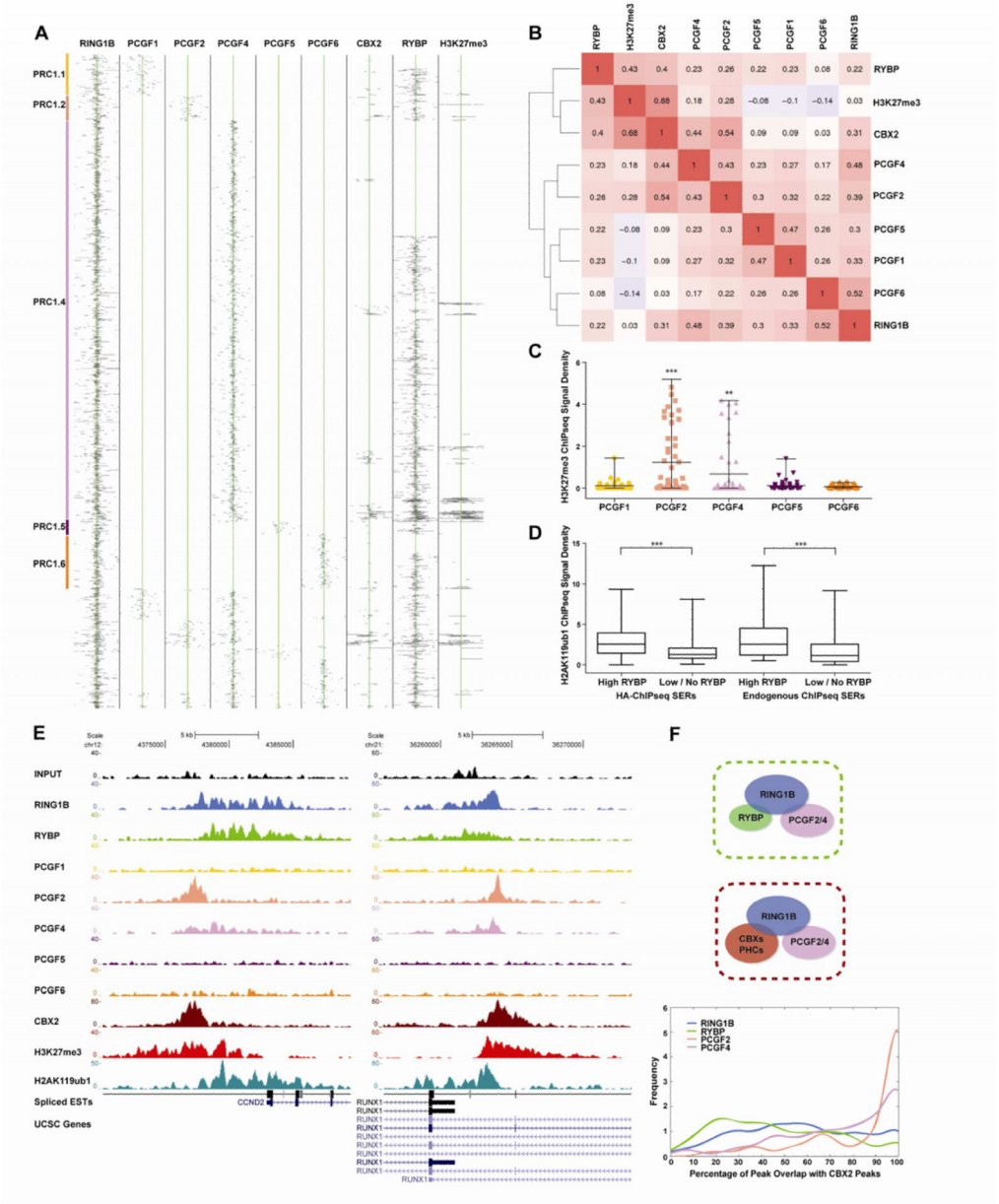

Figure 3. High density map and correlation analysis

A High density map of all the RING1B SERs that are also bound by at least one PCGF. Each horizontal line represents a separate TSS and for each protein the ± 5 kb region is shown, with the position of the TSS marked by the vertical green midline. The position of SERs for the indicated protein is represented by horizontal segments.

B Clustering of the indicated PRC1 components and H3K27me3 according to pairwise Pearson correlation scores of their ChIP-seq signal in the top 1000 RING1B SERs.

C Vertical scatter plot representing H3K27me3 read density (reads per kilo-base per million reads) within the top 50 SERs bound by RING1B and each PCGF. The middle line represents the mean and whiskers mark the range. *P*-values were calculated using one-way ANOVA with Newman-Keuls post-test comparing all pairs of columns. ***, $P<0.001$, **, $P<0.01$ when compared to PCGF1, 5, and 6.

D Vertical box plot representing the H2AK119ub1 read density within top RING1B SERs that overlap with RYBP SERs (“high RYBP”) or have no overlap with RYBP SERs (“low/no RYBP”). The middle line represents the mean and whiskers mark the range. *P*-values were calculated as in (C). ***, $P<0.001$.
E Read density profile for different subunits of PRC1.2, PRC1.4, H3K27me3, and H2AK119ub1 at *CCND2* and *RUNX1*. The x axis corresponds to genomic locations, with the scale and genomic position shown on top. The y axis corresponds to the ChIP-seq signal density. Spliced ESTs and UCSC Genes representation are shown on the bottom.
F Top, a cartoon representing the proposed complex composition. Bottom, extent of peak overlap in regions occupied by RING1B, PCGF2, PCGF4, or RYBP and CBX2. The degree of local overlap of regions enriched for the indicated PRC1 subunit with CBX2-enriched regions is plotted on the x axis, and their frequency is plotted on the y axis.

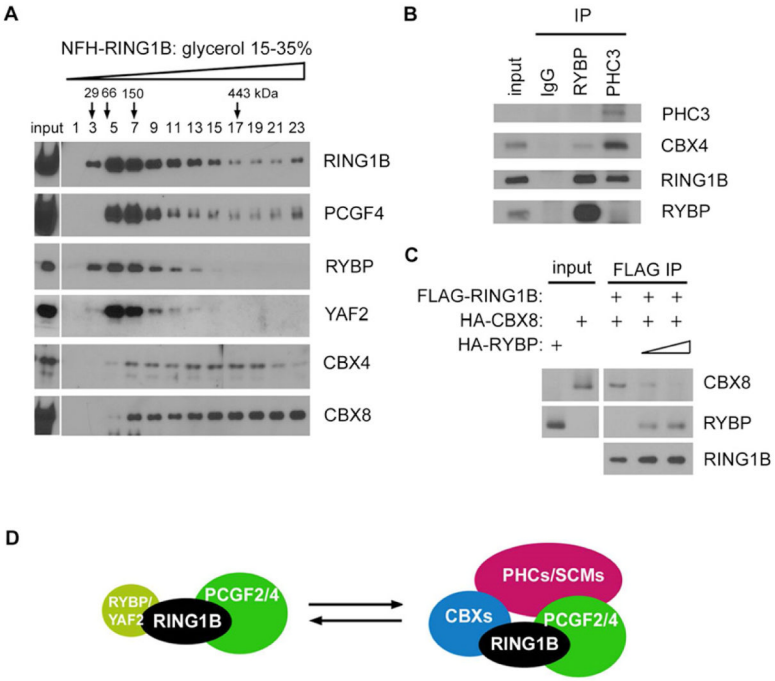

Figure 4. Biochemical isolation of PRC1.4 sub-complexes

A Glycerol gradient analysis of FLAG-purified RING1B complexes. Every other fraction from a 15–35% glycerol gradient was further purified on HA-beads and resolved on SDS-PAGE followed by immunoblotting for the indicated antigens.

B IP of FLAG-purified RING1B complexes by antibodies against RYBP, PHC3, and control IgG. The bound proteins were run on SDS-PAGE and detected with the indicated antibodies.

C Competitive binding assay to test the interaction of FLAG-RING1B with HA-RYBP and HA-CBX8. HA-CBX8 was incubated with FLAG-RING1B in the absence or presence of HA-RYBP and precipitated with FLAG-beads. The bound fraction was resolved on SDS-PAGE and specific proteins revealed by western blot using HA and RING1B antibodies.

D Schematic classification of PRC1.2/1.4 complexes.

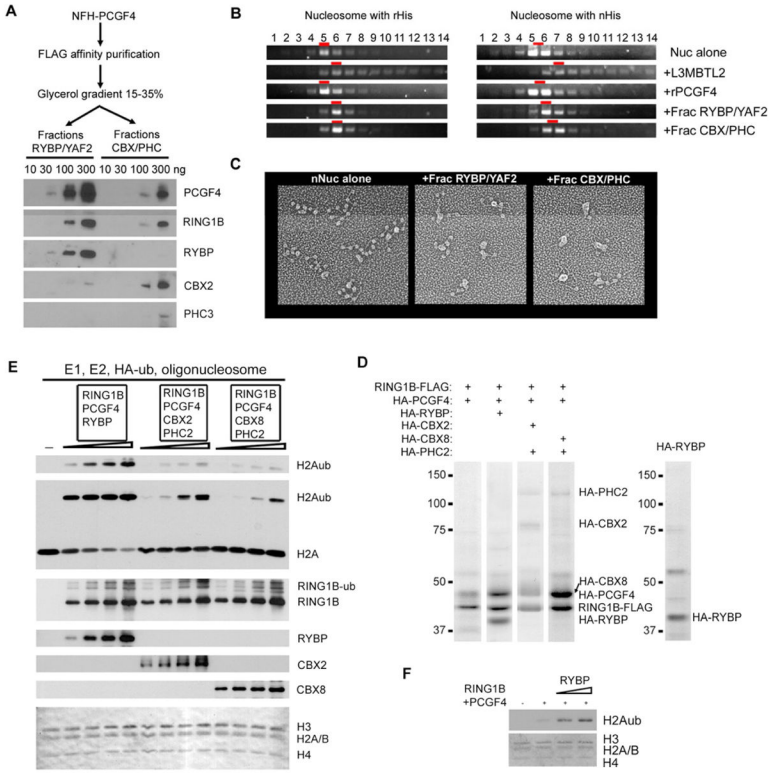

Figure 5. Effect of PRC1.4 complex composition on chromatin compaction and H2AK119 monoubiquitination

A Complexes enriched for RYBP or YAF2 (“Fractions RYBP/YAF2”), or for CBX and PHC proteins (“Fractions CBX/PHC”) were isolated as indicated in the scheme on the top, and examined for their compositions by immunoblotting using antibodies as indicated (bottom).

B Recombinant proteins and protein complexes isolated as in **A** were incubated with nucleosomal arrays. The resulting chromatin compaction was examined by differential centrifugation on a sucrose gradient. The DNA contents of the resulting fractions were visualized on an agarose gel, followed by ethidium bromide staining. The fraction of enriched nucleosomes of each samples are underlined in red.

C The nucleosome-enriched fractions from **B** were visualized by electron microscopy (Experimental Procedures).

D Coomassie staining of reconstituted complexes or recombinant proteins isolated from baculoviruses infected SF9 insect cells.

E Reconstituted complexes were used in an *in vitro* nucleosomal H2A monoubquitinylation assay (Experimental Procedures). The reactions were resolved on SDS-PAGE, followed by immunoblotting. The top two panels show the monoubiquitinated H2A detected by a specific H2AK119ub1 antibody and an H2A antibody, respectively. Components of reconstituted complexes were also shown by western blotting using antibodies against RING1B, RYBP, CBX2, and CBX8, respectively. Note that multiple bands migrate above RING1B, representing ubiquitinated forms of RING1B. Ponceau staining of histones is shown at the bottom.

F Effects of RYBP on E3 ligase activity of reconstituted RING1B- PCGF4 complex toward H2AK119. Varying amounts of RYBP purified from insect cells were used in the *in vitro* H2A monoubquitinylation assay as in **E**, and H2AK119ub1 was detected by immunoblotting.

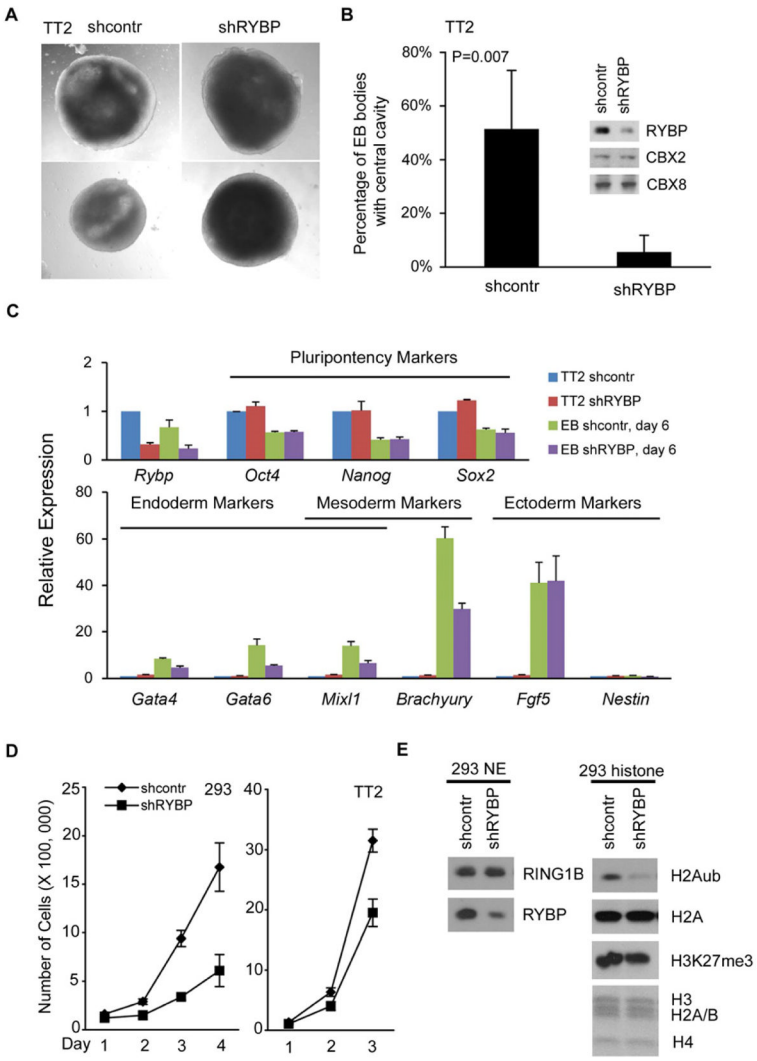

Figure 6. Requirement of RYBP for ES cell differentiation and cell proliferation

A Morphology of embryoid bodies (EBs) formed by TT2 cells with mock or RYBP stable knockdown (Supplemental Experimental Procedures). Note the presence of central cavities in control cells, which was only rarely seen in RYBP knockdown cells.

B Quantification of the percentage of EBs showing central cavities in control or RYBP knockdown TT2 cells. Mean percentages and standard deviations were obtained from four independent experiments for each group. P-value was calculated using a type I, one direction T-test. The insert shows the efficiency and specificity of RYBP knockdown.

C Profiles of expression of pluripotency (top) and differentiation (bottom) marker genes in TT2 cells or EBs after 6 day differentiation, either with mock or RYBP stable knockdown. Expression levels are normalized over those in TT2 cells with mock knockdown. All mean values of expression levels and standard deviations were calculated from three technical replicates. See Supplemental Experimental Procedures for details.

D Growth curve of HEK 293 and TT2 cells with RYBP stable knockdown or mock control. Cells were seeded at 10^5 at day zero, and cell numbers were counted every day. All mean cell numbers and standard deviations were calculated from triplicate experiments.

E The efficiency and specificity of RYBP knockdown in NE were shown by immunoblotting, as well as the effect of RYBP knockdown on H2AK119ub1 using acid-extracted histones from HEK 293 cells in **D**.